A combined photoelectron spectroscopy and relativistic ab initio studies of the electronic structures of UFO and UFO^-

Soumendra K. Roy, Tian Jian, Gary V. Lopez, Wei-Li Li, Jing Su, David H. Bross, Kirk A. Peterson, Lai-Sheng Wang, and Jun Li

Citation: The Journal of Chemical Physics **144**, 084309 (2016); doi: 10.1063/1.4942188
View online: https://doi.org/10.1063/1.4942188
View Table of Contents: http://aip.scitation.org/toc/jcp/144/8
Published by the American Institute of Physics

Articles you may be interested in

Manganese-centered tubular boron cluster – MnB_{16}^-: A new class of transition-metal molecules
The Journal of Chemical Physics **144**, 154310 (2016); 10.1063/1.4946796

Observation and characterization of the smallest borospherene, B_{28}^- and B_{28}
The Journal of Chemical Physics **144**, 064307 (2016); 10.1063/1.4941380

Strong electron correlation in UO_2^-: A photoelectron spectroscopy and relativistic quantum chemistry study
The Journal of Chemical Physics **140**, 094306 (2014); 10.1063/1.4867278

Photoelectron spectroscopy and theoretical studies of gaseous uranium hexachlorides in different oxidation states: UCl_6^{q-} (q = 0–2)
The Journal of Chemical Physics **142**, 134308 (2015); 10.1063/1.4916399

Probing the electronic structures of low oxidation-state uranium fluoride molecules UF_x^- (x = 2-4)
The Journal of Chemical Physics **139**, 244303 (2013); 10.1063/1.4851475

Photoelectron spectroscopy and the electronic structure of the uranyl tetrachloride dianion: $UO_2Cl_4^{2-}$
The Journal of Chemical Physics **137**, 064315 (2012); 10.1063/1.4742062

PHYSICS TODAY
WHITEPAPERS

ADVANCED LIGHT CURE ADHESIVES

Take a closer look at what these environmentally friendly adhesive systems can do

READ NOW

PRESENTED BY
MASTERBOND
ADHESIVES | SEALANTS | COATINGS

A combined photoelectron spectroscopy and relativistic *ab initio* studies of the electronic structures of UFO and UFO^-

Soumendra K. Roy,[1] Tian Jian,[2] Gary V. Lopez,[2] Wei-Li Li,[2] Jing Su,[3] David H. Bross,[4] Kirk A. Peterson,[4,a)] Lai-Sheng Wang,[2,a)] and Jun Li[1,a)]
[1]*Department of Chemistry and Key Laboratory of Organic Optoelectronics and Molecular Engineering of Ministry of Education, Tsinghua University, Beijing 100084, China*
[2]*Department of Chemistry, Brown University, Providence, Rhode Island 02912, USA*
[3]*Shanghai Institute of Applied Physics, Chinese Academy of Sciences, Shanghai 201800, China*
[4]*Department of Chemistry, Washington State University, Pullman, Washington 99164-4630, USA*

(Received 8 November 2015; accepted 28 January 2016; published online 26 February 2016)

The observation of the gaseous UFO^- anion is reported, which is investigated using photoelectron spectroscopy and relativisitic *ab initio* calculations. Two strong photoelectron bands are observed at low binding energies due to electron detachment from the U-7sσ orbital. Numerous weak detachment bands are also observed due to the strongly correlated U-5f electrons. The electron affinity of UFO is measured to be 1.27(3) eV. High-level relativistic quantum chemical calculations have been carried out on the ground state and many low-lying excited states of UFO to help interpret the photoelectron spectra and understand the electronic structure of UFO. The ground state of UFO^- is linear with an O–U–F structure and a $^3H_4$ spectral term derived from a U $7s\sigma^2 5f\varphi^1 5f\delta^1$ electron configuration, whereas the ground state of neutral UFO has a $^4H_{7/2}$ spectral term with a U $7s\sigma^1 5f\varphi^1 5f\delta^1$ electron configuration. Strong electron correlation effects are found in both the anionic and neutral electronic configurations. In the UFO neutral, a high density of electronic states with strong configuration mixing is observed in most of the scalar relativistic and spin-orbit coupled states. The strong electron correlation, state mixing, and spin-orbit coupling of the electronic states make the excited states of UFO very challenging for accurate quantum chemical calculations. © *2016 AIP Publishing LLC.* [http://dx.doi.org/10.1063/1.4942188]

I. INTRODUCTION

Over the last few decades, actinide chemistry has attracted extensive attention in the scientific community because of its important applications in nuclear science and fuel technology.[1] Actinide chemistry is also important in the field of astrophysics, as some of the radioactive isotopes have been used as cosmo-chronometers to determine the lifetime of stars and galaxies.[2] The strong correlation effects of the partially filled shells, e.g., 5f, 6d, 7s, lead to an extensive state mixing and a dense manifold of low-lying excited electronic states[3] for systems that contain one or more actinide atoms. Scalar relativistic (SR) effects and also spin-orbit (SO) coupling have profound influences on the energy levels, as well as the chemical and physical properties in actinide systems.[4–6] On the other hand, the presence of a high density of low-lying electronic states makes the spectra of actinides very difficult to interpret and predict to high accuracy. Therefore, high resolution spectroscopic data as well as rigorous theoretical treatments using high-level relativistic quantum chemical methods are necessary to accurately explain the electronic structure and properties of those systems in which the heavy elements play a significant role.[6]

In the present work, the first observation of the gaseous UFO^- anion is reported and characterized using photoelectron spectroscopy (PES) at two different photon energies. In addition, wavefunction-based multi-configurational *ab initio* calculations of both the anion and its corresponding neutral have been carried out using methods incorporating both scalar and SO coupling relativistic contributions to study the photoelectron spectra in detail. Both species are very interesting due to the strong electron correlation and relativistic effects due to uranium. The UFO^- and UFO systems are isoelectronic with $U(II)F_2$ and $U(III)O_2^-$, respectively, which have been studied extensively.[7–24] Therefore, the photoelectron spectra of UFO^- should be very helpful to obtain information about the ground state as well as low-lying excited states of UFO neutral. Experimental vertical detachment energies (VDEs) are compared with the theoretical calculation of the ground and many low-lying excited electronic states of neutral UFO in order to interpret the experimental findings from the UFO^- spectra.

II. EXPERIMENTAL AND COMPUTATIONAL DETAILS

A. Photoelectron spectroscopy

The experiment was carried out using a magnetic-bottle PES apparatus equipped with a laser vaporization cluster source.[25] The UFO^- anion was produced as a contaminant during experiments on UF_x^- anions.[22] In brief, a uranium

a)Authors to whom correspondence should be addressed. Electronic addresses: kipeters@wsu.edu, Lai-Sheng_Wang@brown.edu, junli@tsinghua.edu.cn.

 © 2016 AIP Publishing LLC

disk target was ablated by a pulsed laser in the presence of a helium carrier gas containing a small amount of F_2. Plasma reactions between the laser-vaporized uranium atoms and F_2 produced various UF_x^- species.[22] However, because of oxide contamination on the target surface, strong UFO^- anion signals were observed along with UF_2^- and UO_2^-, in particular, when a fresh target was used. Clusters from the laser vaporization source were entrained in the Ar/He carrier gas and underwent a supersonic expansion to form a cold and collimated molecular beam after passing a skimmer. Anions from the beam were extracted perpendicularly and analyzed by a time-of-flight mass spectrometer. The UFO^- anions of interest were mass-selected and decelerated before being photodetached by a laser beam at 532 nm (2.331 eV) and 266 nm (4.661 eV) from a Nd-YAG laser. Photoelectrons were analyzed in a 3.5 m long flight tube and the photoelectron spectra were calibrated by the known spectra of Pb^- and Bi^-. The resolution of the apparatus, $\Delta E_k/E_k$, was better than 2.5%, i.e., ~25 meV for 1 eV electrons.

B. Computational details

The quantum chemical calculations were performed using *ab initio* relativistic multi-configurational methods, primarily complete active space second-order perturbation theory (CASPT2), but with two parallel approaches. The first set of calculations utilized the all-electron scalar relativistic second-order Douglas-Kroll-Hess (DKH2) Hamiltonian as implemented in the MOLCAS program, version 7.8.[26,27] These calculations employed the ANO-RCC-VQZP basis set[28] for all atoms. The second series of calculations employed the small-core, 60 electron relativistic pseudopotential (PP) of Dolg and Cao[29] which was adjusted to multiconfiguration Dirac-Hartree-Fock reference data with a perturbative estimate of the Breit interaction, in conjunction with a series of correlation consistent cc-pV*n*Z-PP basis sets[30] on U and the standard aug-cc-pV*n*Z sets on F and O ($n = D$, T, Q).[31,32] These combinations are denoted as V*n*Z-PP below. In both series of calculations (DKH2 and PP), only the semi-core (U 6s and 6p) and valence (U 5f, 6d, 7s and O, F 2s and 2p) electrons were correlated in the CASPT2 calculations.

It should be noted that while the CASPT2 level of theory may not have the accuracy to discern between nearly degenerate electronic states, as in the well-studied $^1\Sigma^+$–$^3\Phi$ splitting in the CUO molecule (see, for example, Ref. 33 and references therein), it has been shown to be reliable for other molecules similar to UFO/UFO^-, e.g., UO_2^- (Ref. 23) and UF/UF^+ (Refs. 34 and 35), as well as even UO_2^{2+} (up to 41 000 cm^{-1} above the ground state).[36,37] In the case of CUO, more accurate results were obtained in Ref. 33 by using the singles and doubles coupled cluster method with perturbative triples along with the Dirac-Coulomb Hamiltonian, DC-CCSD(T), but the UFO system has too much multireference character for this method. Another approach could possibly be the multireference intermediate Hamiltonian Fock Space Coupled Cluster (IH-FSCCSD) method (see, for example, Ref. 19 and references therein), which could also be superior to CASPT2, but this could only be used in molecules with a maximum of 2 open-shell electrons and, therefore, could not be used for either UFO or UFO^-.

Since a series of correlation consistent basis sets were used in the PP-based calculations, it was possible to determine the complete basis set (CBS) limits. The CASSCF CBS limits were obtained by using the Karton and Martin[38] formula with the TZ and QZ energies,

$$E_n^{CAS} = E_{\mathrm{CBS}}^{\mathrm{CAS}} + A\,(n+1)\,e^{-6.57\sqrt{n}}, \tag{1}$$

where the cardinal number of the basis set, n, was used instead of $l_{\max}$, i.e., 3 for TZ and 4 for QZ, as was previously done for the other uranium-containing systems.[30,39] The CASPT2 correlation energies were extrapolated to their CBS limits using TZ and QZ via[40,41]

$$E_n^{corr} = E_{\mathrm{CBS}}^{corr} + \frac{B}{(n+1/2)^4}. \tag{2}$$

1. All-electron DKH2 calculations

At the first stage, a DFT geometry optimization (a trial calculation) in the case of the triplet state of UFO^- was performed to study the pattern of molecular orbital (MO) energy levels relative to the atomic orbitals (AOs) of U, F, and O and also to evaluate the active space orbitals for the final optimization and computations of low-lying electronic states of UFO. The generalized gradient approximation (GGA) with the PBE exchange-correlation functional[42] was used for this purpose. Relativistic effects were included through scalar relativistic ZORA,[43] as implemented in the Amsterdam Density Functional (ADF) program.[44–46] Slater-type basis sets with triple-ζ plus two polarization functions (TZ2P) were used for all atoms.[47] In the case of U, the $1s^2$-$5d^{10}$ orbitals were frozen, while for O and F, the $1s^2$ inner-shell orbitals

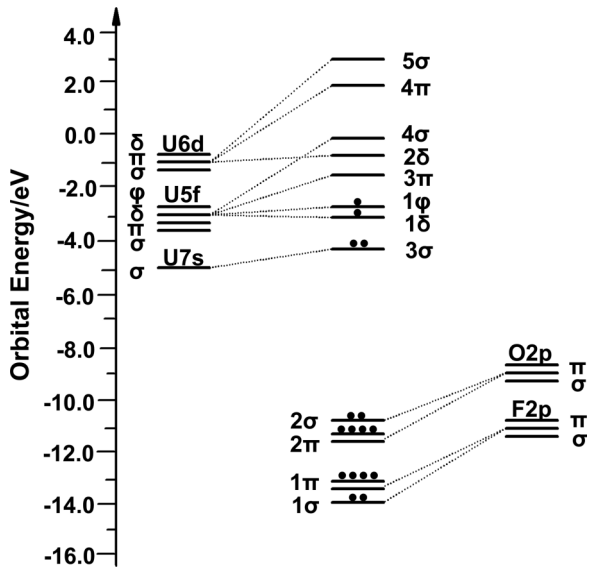

FIG. 1. Qualitative valence MO energy-level scheme of the UFO^- ion at the scalar-relativistic DFT/GGA PBE level. The energy levels of UFO^- have been shifted down by ~4.7 eV to match the energies of the U5f (δ, φ) and 6dδ MOs with the corresponding AOs.

were kept frozen (frozen-core approximation).[48,49] The scalar relativistic PBE energy levels are shown in Figure 1. The thin lines in the figure connect the major contributing AOs with those of the corresponding MO's. The calculation shows that the 1δ, 1φ, and 2δ MOs are quasi-atomic orbitals, that is, these are almost atomic $5f_\delta$, $5f_\varphi$, and $6d_\delta$ orbitals, respectively, with slight ligand perturbations. Therefore, the energy levels of all MO's were shifted down by ~4.7 eV to match their energies with those of the corresponding f_δ and f_φ AOs. The MO energies of 1σ, 1π, 2 σ, and 2 π were raised relative to the corresponding major AOs. Similarly, the energy levels 3σ, 4π, and 5σ were raised, which are due to the interactions of 5fσ, 6dσ, and 6dπ orbitals with the ligands, especially the oxide ion, which is energetically closer to these MO's.

At the second stage, a closed-shell restricted Hartree-Fock (RHF) single-point calculation was performed on $[UFO]^{3+}$ in C_{2v} point group symmetry to generate suitable starting orbitals (as shown in Figure 2) for a CASPT2 geometry optimization of UFO^-. The active space orbitals were chosen based on the DFT calculations described above. Since the 6dπ and 6dσ orbitals are much higher in energy (Figure 1) and the 6dδ orbital is nonbonding, these orbitals were therefore excluded from the active space and the MOs selected were U5fφ (1φ), U5fδ (1δ), U5fπ (3π), U7sσ (3σ), U5fσ (4σ), O2pσ (2σ), and O2pπ (2π), among which 10 electrons were distributed in all possible ways in a CASSCF calculation, which was subsequently followed by a CASPT2 geometry optimization. The numbering of the MOs is listed in Figure 2 and is also discussed with regards to the DFT energy level diagram (Figure 1). Numerical gradients were used for the CASPT2 optimization.[26] The optimization was done for

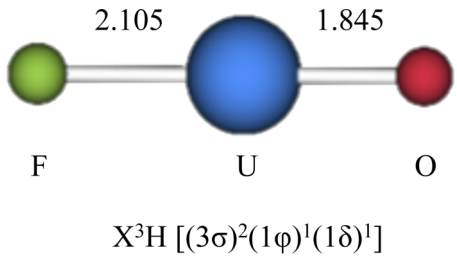

FIG. 3. The optimized structure of UFO^- at the SR/CASPT2 level (DKH2) along with the ground state electronic configuration and bond lengths (in Å). The analogous SR/CASPT2/VQZ-PP bond lengths were 2.101 Å and 1.856 Å for *r*(UF) and *r*(UO), respectively.

all possible spin-multiplicities to determine the lowest energetic state for UFO^-. The resulting ^3H ground state optimized structure of UFO^- at the DKH2-CASPT2 level is shown in Figure 3.

The CASPT2 optimized coordinates of UFO^- were then used to calculate its VDEs and the corresponding excitation energies of many low-lying excited electronic states of neutral UFO. In this regard, single-point state-averaged complete-active space self-consistent field (SA-CASSCF) calculations were first performed for quartet and doublet spin-multiplicities. Since the calculation of VDEs is of interest, which correspond to the low energy region of the photoelectron spectra and also the low-lying electronically excited states of UFO, the active space, therefore, included U5fφ (1φ), U5fδ (1δ), U5fπ (3π), U7sσ (3σ), U5fσ (4σ), U6dδ (2δ), U6dπ (4π), and U6dσ (5σ) MOs, in which 3 electrons were distributed. The SA-CASSCF wave functions for doublet and quartet spin

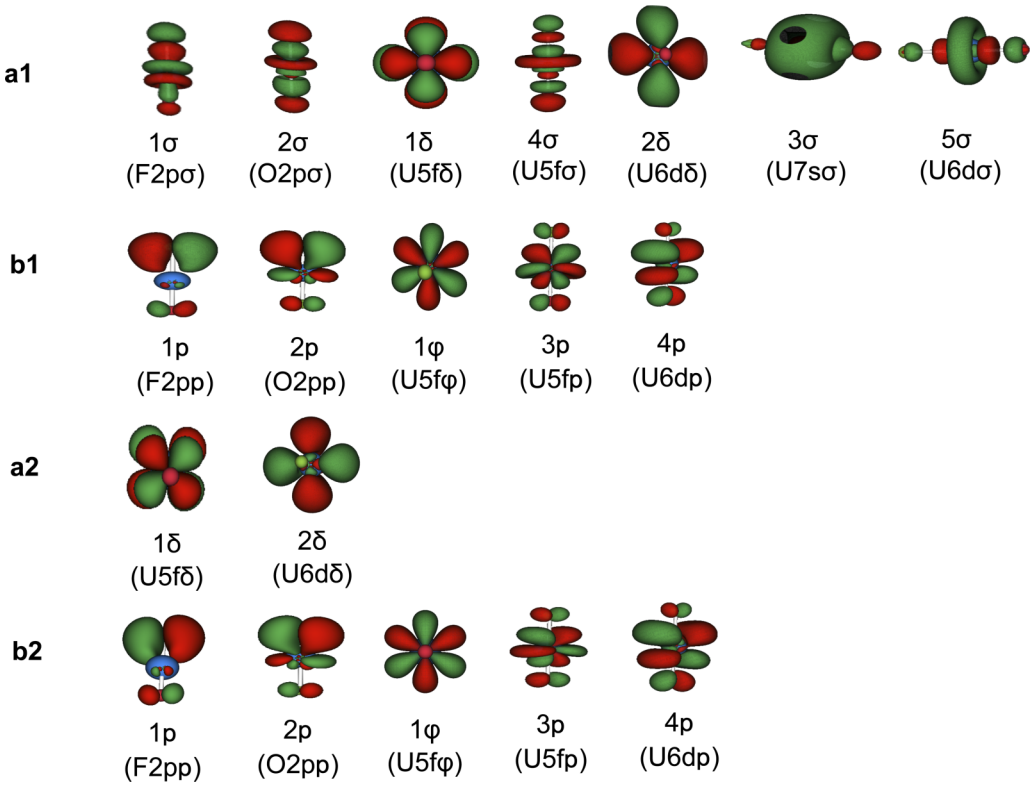

FIG. 2. Contour plots of valence molecular orbitals of the UFO^{3+} ion at the DKH2-RHF level. The numbering of these MO's is in the order of the corresponding MO energy levels in Figure 1.

multiplicities among each irreducible representation of the C_{2v} group were optimized with equal weight for the roots of interest using convergence thresholds of 10^{-7} a.u. (energy), 10^{-4} a.u. (orbital rotation matrix), and 10^{-4} a.u. (energy gradient). The number of roots considered for each symmetry was 10 with overall 40 quartet roots and 40 doublet roots being calculated. The SR effects were included by adding the corresponding terms of the DKH2 Hamiltonian to the one-electron integrals. The dynamic electron correlation effects were studied at the multi-state complete-active space second-order perturbation (MS-CASPT2) level using SA-CASSCF vectors as zeroth-order wave function. The ionization potential-electron affinity (IPEA) shift parameter[50] was adjusted to 0.3 to improve the convergence and also avoid the higher-energy intruder states. At the final stage, the SR spin-free quartet and doublet states obtained at the MS-CASPT2 level were allowed to mix under the influence of the SO Hamiltonian. We used an effective one-electron operator as suggested by Hess and co-workers,[51–53] which simplifies the computation of the SO matrix elements. The SO integrals were calculated by a Douglas-Kroll type atomic mean-field integral (AMFI) approach[51,52] that was used to compute the multi-center one- and two-electron integrals. The SO coupled electronic states were calculated using the complete active-space state interaction (CASSI) program.[26,52]

2. PP-based calculations

The MOLPRO suite of *ab initio* programs[54] was used in relativistic PP-based calculations. Initially, SA-CASSCF calculations were carried out to represent the lowest energy spin-free, ΛS, states. The states were calculated in the highest abelian group available, i.e., C_{2v}. Expectation values of L_z^2 were calculated in all cases to ensure that both degenerate components of each Λ state were correctly included. As above, the CASSCF active space for UFO included 3 electrons in 12 orbitals ($4\times a_1$, $3\times b_1$, $3\times b_2$, $2\times a_2$) that had predominantly U 5f, 6d (δ,π only), and 7s characters, while all lower energy orbitals (including U 6s and 6p, F 2s and 2p, and O 2s and 2p) were constrained to be doubly occupied. Additional higher-lying orbitals, including the 7p of U and beyond, did not appreciably contribute to the CASSCF wavefunctions of UFO. Orbitals with π character mostly resulting from the $7p_x$ and $7p_y$ were found to be partially occupied in UFO^-, but a similar MO was not observed or occupied upon increasing the active space in neutral UFO, while orbitals corresponding to the 6d were not observed. This resulted in a CASSCF active space for UFO^- including 4 electrons in 9 orbitals ($2\times a_1$, $3\times b_1$, $3\times b_2$, $1\times a_2$).

Post-CASSCF calculations were carried out at the CASPT2 level of theory[55] using the same active spaces as the preceding CASSCF calculations. To avoid problems with intruder states in the CASPT2 calculations and to improve convergence, level shifts were utilized using the smallest possible IPEA shift[49] for all included states and geometries. For UFO, this shift corresponded to 0.26, while for UFO^-, it was 0.28.

The state-interacting method for the treatment of SO coupling was used as implemented in MOLPRO [56] to calculate the molecular Ω states. In this method, the SO eigenstates are obtained by diagonalizing $H_{el} + H_{SO}$ in a basis of eigenstates of H_{el}. The matrix elements of H_{SO} are constructed using the SO operator from the U PP. In the present work, the SO matrix elements were calculated throughout at the CASSCF level of theory, whereas the diagonal terms of $H_{el} + H_{SO}$ were replaced by CASPT2 energies. In the cases of molecular states with $\Lambda \neq 0$, the two associated CASPT2 energies were averaged to ensure exact degeneracies. The CASSCF SO matrix elements were calculated using the same basis set as used for the diagonal terms or VQZ-PP when the extrapolated CBS limits for the diagonals were used. In the present work, a total of 18 ΛS electronic states were calculated for UFO, while a total of 31 ΛS electronic states were calculated for UFO^-. After diagonalization of $H_{el} + H_{SO}$, the values of $|\Omega|$ for the molecules were assigned by converting from the Cartesian eigenfunction basis to a spherical basis, and then adding the projection (Σ) of the spin angular momentum S to Λ to obtain $|\Omega|$.

In order to facilitate the calculation of equilibrium geometries and harmonic vibrational frequencies for many of the low-lying SO electronic states, near-equilibrium potential energy surfaces were derived from 28 symmetry-unique geometries distributed about the ground state linear equilibrium geometry with $\Delta r_i = r_i - r_{ie} = -0.3, -0.2, -0.1, 0.0, +0.1, +0.3, +0.5\ a_o$. The calculated energies were accurately fit to polynomials in simple displacement coordinates,

$$E(r_1, r_2) = \sum_{ij} C_{ij} \Delta r_1^i \Delta r_2^j, \tag{3}$$

where i and j ranged from 0 to 5 and $i + j \leq 4$ when both i and j were not equal to 0. The fitting and determination of the spectroscopic constants were carried out with the program SURFIT.[57]

III. RESULTS AND DISCUSSION

A. Photoelectron spectra of UFO^-

The photoelectron spectra of UFO^- are shown in Figure 4 at two different photon energies. Two strong bands labeled as X and A are observed in the low binding energy region of the 532 nm spectrum (Figure 4(a)). Two weak bands labeled as B and C are observed around 2.0 eV. Based on our previous studies for UF_2^- and UO_2^-,[22,23] the intense bands X and A should correspond to electron detachment from the U-based 7sσ orbital of UFO^-, whereas the weak bands B and C may come either from 5f orbitals or from two-electron transitions. The feature X with a VDE of 1.29 eV should correspond to the detachment transition from the anion ground state to that of neutral UFO. The adiabatic detachment energy (ADE) of band X, evaluated from the onset of band X, is 1.27(3) eV, which corresponds to the electron affinity (EA) of neutral UFO. The feature A with a VDE of 1.40 eV should correspond to the detachment transition to the first excited state of UFO. The separation between these two peaks is 0.11 eV (887 cm^{-1}), which should represent the first excitation energy of UFO. The step labeled with * is from a contamination. There is a shoulder around 1.48 eV, separated from band A

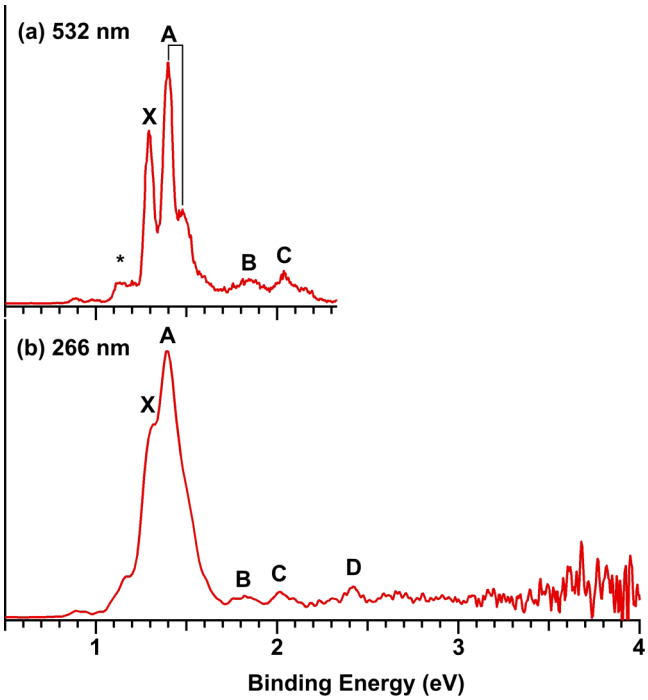

FIG. 4. Photoelectron spectra of UFO^- at (a) 532 nm and (b) 266 nm.

by 640 cm^{-1}, which appears to be a vibrational feature for the first excited state. Our previously observed U–O stretching frequency for UO_2 was 856 cm^{-1},[24] whereas the U–F stretching frequency observed for UF_2 was about 580 cm^{-1}.[22] Thus, the observed vibrational spacing of 640 cm^{-1} in band A is likely due to the U–F stretching mode in UFO. The band B observed at 1.84 eV and band C at 2.04 eV are weak and broad, which may each contain many detachment transitions.

At 266 nm (Figure 4(b)), the bands X and A are not well resolved. An additional weak broad band D at 2.42 eV is observed, which is similar to bands B and C. Nearly continuous weak signals are observed above 2.5 eV, which are similar to those observed in the photoelectron spectra of UF_2^- and UO_2^- due to complicated two-electron transitions.[22,23] The detachment of the F2p and O2p electrons should occur at much higher binding energies beyond the photon energy at 266 nm, as observed in the spectra of UF_2^- and UO_2^-.

B. Theoretical results and comparison with experiment

For the spectral terms or electronic states of molecules with $C_{\infty v}$ symmetry, Σ, Π, Δ, Φ, Γ, H, I, K are used for Λ = 0, 1, 2, 3, 4, 5, 6, 7, respectively, where Λ is the projection of the total orbital angular momentum on the molecular axis. The sum of Λ and the projection of the total spin angular momentum on the molecular axis (Σ) is given by Ω, specifically $\Omega = |\Lambda + \Sigma|$.[58] Even though UFO^- and UFO are linear molecules with $C_{\infty v}$ symmetry, the *ab initio* calculations were performed in its C_{2v} sub-group, in which the σ, π, δ, φ symmetries of the $C_{\infty v}$ group are reduced into a_1, $b_1 + b_2$, $a_1 + a_2$, and $b_1 + b_2$, respectively. The ground-state DKH2-CASPT2 optimized structure of UFO^- is shown in Figure 3. The MO contours of orbitals obtained from a closed-shell DKH2-RHF calculation on the UFO^{3+} ion are shown in Figure 2. In a_1 symmetry, the MOs 1σ, 2σ, and 4σ having $F2p_z$, $O2p_z$, and U7s as major contributions, respectively, are bonding in nature. The MO's U5fφ (1φ) and U6dδ (2δ) are mainly nonbonding, quasi-atomic orbitals, whereas the MO's 4σ and 5σ having U5fσ and 6dσ as major contributions are antibonding in nature. The doubly occupied 3σ bonding orbital involved in the ground state configuration of UFO^- has a major contribution from the U7s orbital with smaller contributions from U6dσ and O2pσ orbitals. In b_1/b_2 symmetry, 1π and 2π orbitals having $F2p_y$, $O2p_y$ as major contributions, respectively, are bonding in nature. The MO U5fφ (1φ) is nonbonding, whereas U5fπ (3π) and U6dπ (4π) are antibonding orbitals. In a_2 symmetry, U5fδ (1δ) and U6dδ (2δ) MOs are nonbonding.

TABLE I. CASSCF/VQZ-PP NBO analyses for the UFO^{3+}, UFO^{2+}, UFO^+, UFO, and UFO^- molecular systems.

	U open-shell orbitals	States[a]	Natural electron configuration[b] and natural charge		
			U	O	F
UFO^{3+}	…	$^1\Sigma^+$	$5f^{1.6}6d^{0.6}$ +3.89	$2s^{2.0}2p^{4.5}$ −0.45	$2s^{2.0}2p^{5.4}$ −0.44
UFO^{2+}	5f	$^2\Phi+^2\Delta$	$5f^{2.2}6d^{0.6}$ +3.27	$2s^{2.0}2p^{4.7}$ −0.68	$2s^{2.0}2p^{5.6}$ −0.59
UFO^+	$5f^2$	$^3H+^3\Gamma+(1)^3\Phi+(2)^3\Phi+^3\Delta+^3\Pi+(1)^3\Sigma^-+(2)^3\Sigma^-+^1H+^1\Gamma+^1\Phi+^1\Pi+^1\Sigma^+$	$5f^{2.6}6d^{0.6}$ +2.80	$2s^{1.9}2p^{5.1}$ −1.04	$2s^{2.0}2p^{5.8}$ −0.76
UFO	$5f^27s$	$^4H+^4\Gamma+^4\Delta+^4\Pi+(1)^4\Sigma^-+(2)^4\Sigma^-+^2H+(1)^2\Gamma+(2)^2\Gamma+(1)^2\Delta+(2)^2\Delta+(1)^2\Pi+(2)^2\Pi+(3)^2\Pi+^2\Sigma^++^2\Sigma^-$	$5f^{2.5}6d^{0.7}7s^{0.8}$ +1.93	$2s^{1.9}2p^{5.2}$ −1.15	$2s^{2.0}2p^{5.8}$ −0.77
UFO^-	$5f^27s^2$	$(1)^3\Gamma+^3\Delta+^3H+(1)^3\Pi+^3\Phi+^3\Sigma^-+(1)^1\Gamma+^1\Sigma^++(1)^1\Delta+(1)^1\Pi$	$5f^{2.5}6d^{0.7}7s^{1.6}7p^{0.2}$ +0.98	$2s^{1.9}2p^{5.3}$ −1.20	$2s^{2.0}2p^{5.8}$ −0.78

[a]The density matrices and orbitals of these states were averaged and then analyzed.
[b]Any contributions smaller than 0.05 are not shown.

TABLE II. SR/MS-CASPT2 spin-free vertical excitation energies of UFO at the optimized geometry of UFO^-. The active space includes U-5fσ, 5fπ, 5fδ, 5fφ, 6dσ, 6dπ, 6dδ, and U7sσ orbitals.

Term	ΔE (eV)	ΔE (cm^{-1})	Important configurations (leading configurations are in bold-face letters)
$(1)^4H$	0.000	0	**1φ1δ3σ (5fφ5fδ7s)**
$(1)^2H$	0.118	953	**1φ1δ3σ (5fφ5fδ7s)**
$(1)^4\Sigma^-$	0.304	2 456	$1\varphi^2 3\sigma\,(5f\varphi^2 7s) + 1\delta^2 3\sigma\,(5f\delta^2 7s) + 1\delta 2\delta 3\sigma\,(5f\delta 6d\delta 7s)$
$(1)^2\Sigma^-$	0.376	3 035	**$1\delta^2 3\sigma$ ($5f\delta^2 7s$)** + $1\varphi^2 3\sigma\,(5f\varphi^2 7s) + 3\pi^2 3\sigma\,(5f\pi^2 3\sigma)$
$(1)^4\Pi$	0.383	3 092	**1φ1δ3σ (5fφ5fδ7s)** + $1\delta 3\pi 3\sigma\,(5f\delta 5f\pi 7s)$
$(1)^2\Pi$	0.525	4 239	**1φ1δ3σ (5fφ5fδ7s)** + $1\delta 3\pi 3\sigma\,(5f\delta 5f\pi 7s)$
$(1)^4K$	0.689	5 563	**1φ1δ2δ (5fφ5fδ6dδ)**
$(1)^4\Gamma$	0.879	7 091	**1φ3π3σ (5fφ5fπ7s)**
$(1)^2\Gamma$	0.884	7 133	$1\delta^2 3\sigma\,(5f\delta^2 7s) + 1\varphi 3\pi 3\sigma\,(5f\varphi 5f\pi 7s)$
$(2)^4\Gamma$	0.905	7 300	**1φ3π3σ (5fφ5fπ7s)** + $1\varphi 1\delta 3\pi\,(5f\varphi 5f\delta 5f\pi)$
$(1)^2\Sigma^+$	0.907	7 317	$1\varphi^2 3\sigma\,(5f\varphi^2 7s) + 1\delta^2 3\sigma\,(5f\delta^2 7s) + 1\delta 2\delta 3\sigma\,(5f\delta 6d\delta 7s)$
$(2)^2\Pi$	0.933	7 523	**1φ1δ3σ (5fφ5fδ7s)** + $1\delta 3\pi 3\sigma\,(5f\delta 5f\pi 7s)$
$(2)^2\Gamma$	0.949	7 662	$1\delta^2 3\sigma\,(5f\delta^2 7s) + 1\varphi 3\pi 3\sigma\,(5f\varphi 5f\pi 7s) + 1\delta 2\delta 3\sigma\,(5f\delta 6d\delta 7s)$
$(1)^4\Delta$	1.000	8 067	**1φ3π3σ (5fφ5fπ7s)**
$(3)^2\Gamma$	1.015	8 188	**1φ3π3σ (5fφ5fπ7s)** + $1\delta^2 3\sigma\,(5f\delta^2 7s)$
$(2)^4\Delta$	1.028	8 297	**1φ3π3σ (5fφ5fπ7s)**
$(4)^2\Gamma$	1.066	8 601	**1φ3π3σ (5fφ5fπ7s)**
$(1)^4\Phi$	1.070	8 630	**1δ3π3σ (5fδ5fπ7s)** + $1\varphi 1\delta 2\delta\,(5f\varphi 5f\delta 6d\delta)$
$(3)^4\Gamma$	1.078	8 695	$1\varphi 1\delta 3\pi\,(5f\varphi 5f\delta 5f\pi) + 1\varphi 2\delta 3\pi\,(5f\varphi 5f + 6d\delta 5f\pi)$
$(1)^2\Delta$	1.1587	9 347	**1φ3π3σ (5fφ5fπ7s)**
$(1)^2\Phi$	1.172	9 455	**1φ1δ2δ (5fφ5fδ6dδ)** + $1\delta 3\pi 3\sigma\,(5f\delta 5f\pi 7s)$
$(2)^4\Phi$	1.219	9 837	**1φ1δ2δ (5fφ5fδ6dδ)** + $1\delta 3\pi 2\delta\,(5f\delta 5f\pi 6d\delta)$
$(3)^4\Delta$	1.236	9 968	$1\varphi^2 2\delta\,(5f\varphi^2 6d\delta) + 1\delta^2 2\delta\,(5f\delta^2 6d\delta) + 1\delta 2\delta^2\,(5f\delta 6d\delta^2)$
$(2)^2\Delta$	1.239	9 996	**1φ3π3σ (5fφ5fπ7s)**
$(4)^4\Delta$	1.279	10 317	$1\varphi^2 2\delta\,(5f\varphi^2 6d\delta) + 1\delta^2 2\delta\,(5f\delta^2 6d\delta) + 1\delta 2\delta^2\,(5f\delta 6d\delta^2)$
$(3)^4\Phi$	1.332	10 742	**1φ1δ2δ (5fφ5fδ6dδ)** + $1\delta 3\pi 3\sigma\,(5f\delta 5f\pi 7s)$
$(2)^4\Sigma^-$	1.386	11 181	$1\varphi^2 3\sigma\,(5f\varphi^2 7s) + 3\pi^2 3\sigma\,(5f\pi^2 7s) + 1\delta^2 3\sigma\,(5f\delta^2 7s)$
$(4)^4\Gamma$	1.413	11 400	**1φ1δ3π (5fφ5f + 6dδ5fπ)** + $1\varphi 3\pi 2\delta\,(5f\varphi 5f\delta 5f\pi)$
$(2)^2\Phi$	1.438	11 597	**1δ3π3σ (5fδ5fπ7s)** + $1\varphi 1\delta 2\delta\,(5f\varphi 5f\delta 6d\delta)$
$(2)^4\Pi$	1.452	11 712	**1φ1δ2δ (5fφ5fδ6dδ)** + $1\delta 3\pi 3\sigma\,(5f\delta 5f\pi 7s)$
$(1)^4I$	1.493	12 045	**1φ3π2δ (5fφ5fπ6dδ)**
$(3)^2\Delta$	1.496	12 071	$1\varphi 3\pi 3\sigma\,(5f\varphi 5f\pi 7s) + 1\delta^2 2\delta\,(5f\delta^2 6d\delta) + 1\varphi^2 2\delta\,(5f\varphi^2 6d\delta)$
$(2)^2\Sigma^-$	1.497	12 075	$1\varphi^2 3\sigma\,(5f\varphi^2 7s) + 1\delta^2 3\sigma\,(5f\delta^2 7s) + 3\pi^2 3\sigma\,(5f\pi^2 7s)$
$(4)^2\Delta$	1.535	12 386	$1\delta^2 2\delta\,(5f\delta^2 6d\delta) + 1\varphi 3\pi 3\sigma\,(5f\varphi 5f\pi 7s) + 1\varphi 3\pi 2\delta\,(5f\varphi 5f\pi 6d\delta)$
$(5)^2\Delta$	1.541	12 429	**1φ3π3σ (5fφ5fπ7s)** + $1\delta 2\delta 3\sigma\,(5f\delta 6d\delta 7s) + 1\delta^2 2\delta\,(5f\delta^2 6d\delta)$
$(1)^2I$	1.558	12 572	**$1\varphi^2 3\sigma$ ($5f\varphi^2 7s$)** + $1\varphi 3\pi 2\delta\,(5f\varphi 5f\pi 6d\delta)$
$(2)^4I$	1.559	12 572	**1φ3π1δ (5fφ5fπ6dδ**) + $1\varphi 2\delta 3\pi\,(5f\varphi 5f + 6d\delta 5f\pi)$
$(5)^4\Delta$	1.583	12 771	$1\varphi^2 2\delta\,(5f\varphi^2 6d\delta) + 1\varphi 3\pi 2\delta\,(5f\varphi 5f\pi 6d\delta) + 3\pi^2 2\delta\,(5f\pi^2 6d\delta)$
$(6)^2\Delta$	1.596	12 877	$1\delta^2 2\delta\,(5f\delta^2 6d\delta) + 1\varphi 3\pi 3\sigma\,(5f\varphi 5f\pi 7s) + 1\varphi^2 1\delta\,(5f\varphi^2 5f\delta)$
$(2)^2I$	1.628	13 130	**$1\varphi^2 3\sigma$ ($5f\varphi^2 7s$)** + $1\varphi 3\pi 2\delta\,(5f\varphi 5f\pi 6d\delta) + 1\delta^2 2\delta\,(5f\delta^2 6d\delta)$
$(3)^2\Phi$	1.632	13 165	**1φ1δ2δ (5fφ5fδ6dδ)** + $1\delta 3\pi 2\delta\,(5f\delta\ 5f\pi 6d\delta) + 1\varphi 3\sigma 4\sigma\,(5f\varphi\ 5f\sigma 7s) + 1\varphi 3\sigma^2\,(5f\varphi 7s^2) + 1\varphi 1\delta^2\,(5f\varphi 5f\delta^2)$
$(6)^4\Delta$	1.672	13 491	**1φ1δ3π (5fφ5f+6dδ5fπ)** + $1\varphi^2 2\delta\,(5f\varphi^2\ 6d\delta) + 3\pi^2 2\delta\,(5f\pi^2 6d\delta)$
$(4)^2\Phi$	1.690	13 635	**1φ1δ2δ (5fφ5fδ6dδ)**
$(5)^2\Phi$	1.698	13 700	**1φ1δ2δ (5fφ5fδ6dδ)** + $1\delta 3\pi 3\sigma\,(5f\delta 5f\pi 7s) + 1\varphi 1\delta 3\sigma\,(5f\varphi 5f\delta 7s)$
$(3)^4\Pi$	1.706	13 764	**1δ3π3σ (5fδ5fπ7s)** + $1\varphi 1\delta 3\sigma\,(5f\varphi 5f\delta 7s) + 1\delta 3\pi 2\delta\,(5f\delta 5f\pi 6d\delta)$
$(5)^4\Gamma$	1.773	14 304	**1φ3π2δ (5fφ5fπ6dδ)**
$(7)^4\Delta$	1.806	14 568	**1φ3π1δ (5fφ5fπ6dδ)** + $1\varphi 3\pi 2\delta\,(5f\varphi 5f\pi 6d + 5f\delta) + 1\varphi 3\pi 1\delta\,(5f\varphi 5f\pi 5f + 6d\delta)$
$(3)^2\Pi$	1.843	14 860	$1\delta 3\pi 3\sigma\,(5f\delta 5f\pi 7s) + 1\varphi 1\delta 2\delta\,(5f\varphi 5f\delta 6d\delta) + 1\delta 3\pi 2\delta\,(5f\delta 5f\pi 6d\delta)$
$(7)^2\Delta$	1.860	15 003	$1\delta^2 1\delta\,(5f\delta^2 6d\delta) + 1\varphi 3\pi 2\delta\,(5f\varphi 5f\pi 6d\delta) + 1\delta^2 2\delta\,(5f\delta^2 6d\delta)$
$(8)^2\Delta$	1.880	15 164	$1\varphi 3\pi 2\delta\,(5f\varphi 5f\pi 6d\delta) + 1\delta^2 2\delta\,(5f\delta^2 6d\delta) + 1\varphi^2 2\delta$
$(3)^2I$	1.891	15 249	$1\delta^2 2\delta\,(5f\delta^2 6d\delta) + 1\varphi^2 3\sigma\,(5f\varphi^2 7s) + 1\varphi 3\pi 2\delta\,(5f\varphi 5f\pi 6d\delta)$

TABLE II. (*Continued.*)

Term	ΔE (eV)	ΔE (cm^{-1})	Important configurations (leading configurations are in bold-face letters)
$(2)^2H$	1.911	15 415	**1φ1δ3σ (5fφ5fδ7s)**
$(2)^4H$	1.956	15 783	**1δ3π2δ (5fδ5fπ6dδ)**
$(4)^2I$	1.963	15 835	$1φ^2 3σ$ (5fφ²7s) + $1δ^2 2δ$ (5fδ²6dδ) + 1φ3π2δ (5fφ5fπ6dδ)
$(3)^4Σ^-$	1.981	15 976	**1φ3π2δ (5fφ5fπ6dδ)**
$(8)^4Δ$	1.983	15 997	**1φ3π2δ (5fφ5fπ6dδ)** $+3π^2 2δ$ (5fπ²6dδ) + $1δ^2 2δ$ (5fδ²6dδ)
$(1)^4Σ^+$	2.051	16 544	**1φ3π2δ (5fφ5fπ6dδ)** + 1φ1δ3π (5fφ5f+6dδ5fπ) + 22%1φ3π2δ (5fφ5fπ6d+5fδ)
$(9)^4Δ$	2.069	16 695	$3π^2 2δ$ (5fπ²6dδ) + 1φ3π2δ (5fφ5fπ6dδ) + $1φ^2 2δ$ (5fφ²6dδ)
$(9)^2Δ$	2.140	17 261	**1φ3π2δ (5fφ5fπ6dδ)**
$(4)^4Π$	2.165	17 465	**1δ3π2δ (5fδ5fπ6dδ)** + 1δ3π3σ (5fδ5fπ7s)

A natural bond orbital (NBO) analysis,[59] carried out at the CASSCF/VQZ-PP level of theory and consisting of natural electron populations and natural charges, for the sequence of molecules UFO^{3+}, UFO^{2+}, UFO^+, UFO, and UFO^- is shown in Table I. For the last four species, the open shell MOs of the ground states correspond to primarily $5f^1$, $5f^2$, $5f^27s^1$, and $5f^27s^2$ configurations on the U center, respectively. The open shell characters for UFO^+ and UFO ($5f^2$ and $5f^27s^1$, respectively) are in contrast to the cases of UO_2 and UO_2^-, which involve the 5f7s and $5f7s^2$ configurations, respectively. This difference is mainly due to the weaker ligand field of the F^- ligand compared to O^{2-}. While the charge on the uranium center is reduced from +3.9 in UFO^{3+} to +3.3 in UFO^{2+} upon occupation of the first 5f MO, adding a second electron (to a second 5f MO) to form UFO^+ only reduces the charge further to +2.8. About half of the charge of the added electron is transferred to O and F 2p orbitals, with the majority being to O 2p. The latter is sequentially reduced upon attaching electrons to UFO^{3+} from −0.45 (UFO^{3+}) to −0.68 (UFO^{2+}) and −1.04 (UFO^+), respectively. Addition of the next two electrons to form UFO and UFO^-, respectively, nearly exclusively involves reducing the oxidation state of the U atom with little change of the natural charge on either the F or O centers. In all the five species, there is a strong contribution from the U 6d orbitals, about 0.6 electrons, while the U 7p makes small contributions to the bonding in the anion.

The ground state electronic configuration of UFO^- at the SR/CASPT2 level is X^3H ($3σ^2 1φ^1 1δ^1$). The CASPT2 U–O bond length using the ANO-RCC-VQZP basis set is 1.845 Å, which is 0.022 Å larger than the U–O bond length in UO_2^-, as reported previously at the SR/CCSD(T) level[23] and 0.017 Å longer than that at the DFT/B3LYP level,[9,23] partly due to the U(II) oxidation state in UFO^-. On the other hand, the U–F bond length of the present calculation is 2.105 Å, which is 0.051 Å longer than the U–F bond length in UF_2 (an isoelectronic species) and 0.013 Å larger than that in the corresponding UF_2^- anion, which was calculated using the PBE functional with the SO-ZORA Hamiltonian by Li *et al.*[22] The different molecular environments and the use of different basis sets and electron correlation methods cause different bond lengths in these three anionic systems. The ∠FUF bond angles in UF_2^- and in UF_2 are 105.2° and 101.7°, respectively, in comparison to the linear UFO bond angle in UFO^-. The linearity of the OUF^- structure is due to the π-interactions among the three atoms, resulting in a double bond between O and U. Also as noted above, the electron configuration of the U atom in OUF^- is approximately $4f^27s^2$, whereas it is $4f^37s^1$ in UF_2. In addition, the CASPT2/VQZ-PP equilibrium geometry of UFO^- is nearly identical to the DKH2 result for the UF distance, 2.101 Å (PP) vs. 2.105 Å (DK), but the UO distance shows more sensitivity to method, 1.856 Å (PP) vs. 1.845 Å (DK).

The interpretation of the photoelectron spectra of UFO^- is the major focus of the present discussion. At the ground state geometry of UFO^-, SR/MS-CASPT2 and SO calculations have been carried out for the ground state and several low-lying electronic excited states of neutral UFO, as shown in Tables II and III, respectively. At the SR/MS-CASPT2 level, a total of 80 spin-free states below 2.2 eV in energy have been found, as given in Table II. The assignments of these SR states, as well as the resulting SO states, have been performed on the basis of standard quantum selection rules and also the transition dipole moments, oscillator strengths, and Einstein A-coefficients.[60,61] The SO-PP results shown in Table III were assigned as discussed above, based in part on L_z^2 eigenvalues, and have been matched to the DKH2 results by comparison of their ΛS character. The SR ground state has been found to be X^4H ($1φ1δ3σ$) for UFO, whereas the first excited state $(1)^2H$ that arises from the same configuration as the ground state lies at 953 cm^{-1} (0.118 eV). The excited states lie very close to each other and the energy differences among most of the coupled excited states are less than 0.05 eV. Most of these low-lying states correspond to a U atomic configuration of $5f^27s$ (see also Table I). Besides the ground state configuration, many other configurations like $1φ1δ2δ$, $1φ3π3σ$, $1φ^2 2δ$, $1φ^2 2δ$, $1φ3π2δ$, etc., also contribute to several excited states due to strong multi-configurational mixing. In some states, such as a $^4Σ^-$ (at 0.304 eV), $a^2Γ$ (at 0.884 eV), there are strong configuration mixings, as shown in Table II.

Table III shows 80 SO-states of UFO below 2.7 eV. The lowest few Ω states are plotted in Figure 5 as a function of the UO and UF distances. The ground state of UFO is found to be $X^4H_{7/2}$ with very small contributions from the $^2Γ$ states.

TABLE III. The experimental and calculated VDEs of UFO^- and the excitation energies (ΔE)[a] of neutral UFO at the MS-CASPT2/SO (DK) and SO-CASPT2/CBS-PP (PP) level.[b] All energies are in eV.

Feature	VDE (expt.)[c]	VDE (DK)	ΔE (DK)	ΔE (PP)	Ω	Composition of SR/MS-CASPT2 spin-free states (leading configurations are in bold-faced letters)
X	1.29(3)	1.29[d]	0.000	0.000	7/2	90% $(1)^4$ H (**1φ1δ3σ**) + 2% $(1)^2\Gamma$ ($1\delta^2 3\sigma + 1\varphi 3\pi 3\sigma$) + 2% $(2)^2\Gamma$ ($1\delta^2 3\sigma + 1\varphi 3\pi 3\sigma + 1\delta 2\delta 3\sigma$)
A	1.40(3)	1.359	0.069	0.082	9/2	52% $(1)^2$H (**1φ1δ3σ**) + 36% $(1)^4$H (**1φ1δ3σ**) + 4% $(1)^2\Gamma$ ($1\delta^2 3\sigma + 1\varphi 3\pi 3\sigma$)
		1.646	0.356	0.342	1/2	41% $(1)^4\Sigma^-$ ($1\varphi^2 3\sigma + 1\delta^2 3\sigma + 1\delta 2\delta 3\sigma$) + 30%$(1)^4\Pi$ (**1φ1δ3σ** + $1\delta 3\pi 3\sigma$) + 13%$^2\Sigma^+$ ($1\varphi^2 3\sigma + 1\delta^2 3\sigma + 1\delta 2\delta 3\sigma$) + 10%$(1)^2\Sigma^-$ (**1δ²3σ** + $1\varphi^2 3\sigma + 3\pi^2 3\sigma$)
B	1.84(4)	1.788	0.498	0.534	11/2	92% ^{4}K (**1φ1δ2δ**)
		1.796	0.506	0.512	3/2	42% $(1)^4\Pi$ (**1φ1δ3σ** + $1\delta 3\pi 3\sigma$) + 21%$(1)^4\Sigma^-$ ($1\varphi^2 3\sigma + 1\delta^2 3\sigma + 1\delta 2\delta 3\sigma$) + 16%$(2)^2\Pi$ ($1\varphi 1\delta 3\sigma + 1\delta 3\pi 3\sigma$)
		1.806	0.516	0.535	1/2	36% $(1)^4\Pi$ (**1φ1δ3σ** + $1\delta 3\pi 3\sigma$) + 19%$(1)^2\Sigma^-$ (**1δ²3σ** + $1\varphi^2 3\sigma + 3\pi^2 3\sigma$) + 18%$(1)^2\Pi$ (**1φ1δ3σ** + $1\delta 3\pi 3\sigma$)
		2.013	0.723	0.680	9/2	72% $(1)^4$H (**1φ1δ3σ**) + 24%$(1)^2$H (**1φ1δ3σ**)
		2.015	0.725	0.690	11/2	58% $(1)^4$H (**1φ1δ3σ**) + 39%$(1)^2$H (**1φ1δ3σ**)
C	2.04(4)	2.279	0.989	1.008	5/2	30% $(1)^2\Phi$ (**1φ1δ2δ** + $1\delta 3\pi 3\sigma$) + 16%$(1)^4\Gamma$ (**1φ3π3σ**) + 15%$(2)^4\Gamma$ (**1φ3π3σ** + $1\varphi 1\delta 3\pi$) + 10%$(2)^4\Phi$ (**1φ1δ2δ** + $1\delta 3\pi 2\delta$)
		2.321	1.031	1.050	5/2	34% $(1)^4\Pi$ (**1φ1δ3σ** + $1\delta 3\pi 3\sigma$) + 11%$(1)^4\Gamma$ (**1φ3π3σ**) + 11%$(2)^4\Gamma$ (**1φ3π3σ** + $1\varphi 1\delta 3\pi$) + 9%$(1)^4\Delta$ (**1φ3π3σ**)
		2.347	1.057	1.050	3/2	70% $(1)^4\Pi$ (**1φ1δ3σ** + $1\delta 3\pi 3\sigma$) + 28%$(1)^2\Pi$ (**1φ1δ3σ** + $1\delta 3\pi 3\sigma$) + 3%$(1)^4\Sigma^-$ ($1\varphi^2 3\sigma + 1\delta^2 3\sigma + 1\delta 2\delta 3\sigma$)
		2.353[e]		1.029	13/2	82% ^{4}K (**1φ1δ2δ**) + 2%^{4}I (**1φ3π2δ**)
		2.376	1.086	1.057	1/2	18% $(1)^4\Pi$ (**1φ1δ3σ** + $1\delta 3\pi 3\sigma$) + 14%$(1)^4\Delta$ (**1φ3π3σ**) + 7% $(1)^4\Sigma^-$ ($1\varphi^2 3\sigma + 1\delta^2 3\sigma + 1\delta 2\delta 3\sigma$) + 6%$(1)^2\Pi$ ($1\varphi 1\delta 3\sigma + 1\delta 3\pi 3\sigma$)
		2.385	1.095	1.131	5/2	30% $(1)^4\Pi$ (**1φ1δ3σ** + $1\delta 3\pi 3\sigma$) + 15%$(1)^4\Gamma$ (**1φ3π3σ**) + 14%$(2)^4\Gamma$ (**1φ3π3σ** + $1\varphi 1\delta 3\pi$) + 7%$(1)^4\Delta$ (**1φ3π3σ**)
		2.392	1.102	1.088	3/2	62% $(1)^4\Sigma^-$ ($1\varphi^2 3\sigma + 1\delta^2 3\sigma + 1\delta 2\delta 3\sigma$) + 14%$(2)^2\Pi$ (**1φ1δ3σ** + $1\delta 3\pi 3\sigma$) + 3%$(2)^2\Delta$ (**1φ3π3σ**) + 3%$(1)^2\Delta$ ($1\varphi 3\pi 3\sigma + 3\Pi^2 1\delta + 1\delta^2 2\delta$)
D	2.42(6)	2.422	1.132	1.092	1/2	44% $(1)^2\Sigma^-$ (**1δ²3σ** + $1\varphi^2 3\sigma + 3\pi^2 3\sigma$) + 28%$(1)^4\Sigma^-$ ($1\varphi^2 3\sigma + 1\delta^2 3\sigma + 1\delta 2\delta 3\sigma$) + 14%$(2)^2\Pi$ (**1φ1δ3σ** + $1\delta 3\pi 3\sigma$) + 4%$(1)^4\Delta$ (**1φ3π3σ**)
		2.454	1.164	1.130	7/2	23% $(1)^4\Gamma$ (**1φ3π3σ**) + 21%$(3)^2\Gamma$ (**1φ3π3σ** + $1\delta^2 3\sigma$) + 20%$(4)^2\Gamma$ (**1φ3π3σ**) + 20%$(2)^4\Gamma$ (**1φ3π3σ** + $1\varphi 1\delta 3\pi$) + 3%$(1)^2\Gamma$ ($1\delta^2 3\sigma + 1\varphi 3\pi 3\sigma$)
		2.496	1.206	1.275	3/2	35% $(1)^2\Pi$ (**1φ1δ3σ** + $1\delta 3\pi 3\sigma$) + 9%$(3)^4\Delta$ ($1\varphi^2 2\delta + 1\delta^2 2\delta + 1\varphi 2\delta^2$) + 9%$(5)^4\Delta$ ($1\varphi^2 2\delta + 1\delta^2 2\delta + 1\delta 2\delta^2$) + 5%$(2)^4\Phi$ (**1φ1δ2δ** + $1\delta 3\pi 2\delta$)
		2.548	1.258	1.251	13/2	94% $(1)^4$H (**1φ1δ3σ**) + 3%$(1)^2$I (**1φ²3σ** + $1\varphi 3\pi 2\delta$) + 2%$(2)^2$I (**1φ²3σ** + $1\varphi 3\pi 2\delta + 1\delta^2 2\delta$)
		2.615	1.325	1.318	1/2	24% $(1)^4\Pi$ (**1φ1δ3σ** + $1\delta 3\pi 3\sigma$) + 18%$^2\Sigma^+$ ($1\varphi^2 3\sigma + 1\delta^2 3\sigma + 1\delta 2\delta 3\sigma$) + 14%$(1)^2\Pi$ (**1φ1δ3σ** + $1\delta 3\pi 3\sigma$)
		2.619	1.329		5/2	16% $(3)^2\Phi$ (**1φ1δ2δ** + $1\delta 3\pi 2\delta + 1\varphi 3\sigma 3\sigma + 1\varphi 3\sigma^2 + 1\varphi 1\delta^2$) + 16%$(3)^4\Phi$ (**1φ1δ2δ** + $1\delta 3\pi 3\sigma$) + 8%$(1)^4\Pi$ (**1φ1δ3σ** + $1\delta 3\pi 3\sigma$)

[a]Calculated at the equilibrium geometry of the anion.
[b]Results for VDEs greater than 2.62 eV are given in Table S5 of the supplementary material.[64]
[c]The number in the parentheses represents the experimental uncertainty.
[d]The ground state energy is adjusted to the experimental first VDE, calculated at 1.234 eV in the PP calculation.
[e]2% $(2)^4\Delta$ (**1φ3π3σ**) and 2% $(1)^4\Pi$ (**1φ1δ3**σ + $1\delta 3\pi 3\sigma$) are mixed with ^{4}K and ^{4}I states due to symmetry breaking, because the calculation was carried out in lower symmetry C_{2v} instead of $C_{\infty v}$.

The ground state of UFO^- has been calculated to be X^3H_4 with the nearest excited state corresponding to Ω = 0 arising from a mixture of $^3\Sigma^-$ and $^3\Pi$ ΛS states and lying 3256 cm^{-1} above the ground state. The calculated first VDE (1.234 eV) corresponds to the transition UFO^- (X^3H_4) → UFO ($X^4H_{7/2}$) and the value given in Table III has been adjusted to match the experimental value of 1.29 eV for better comparison of theoretical and experimental values for excited UFO states.

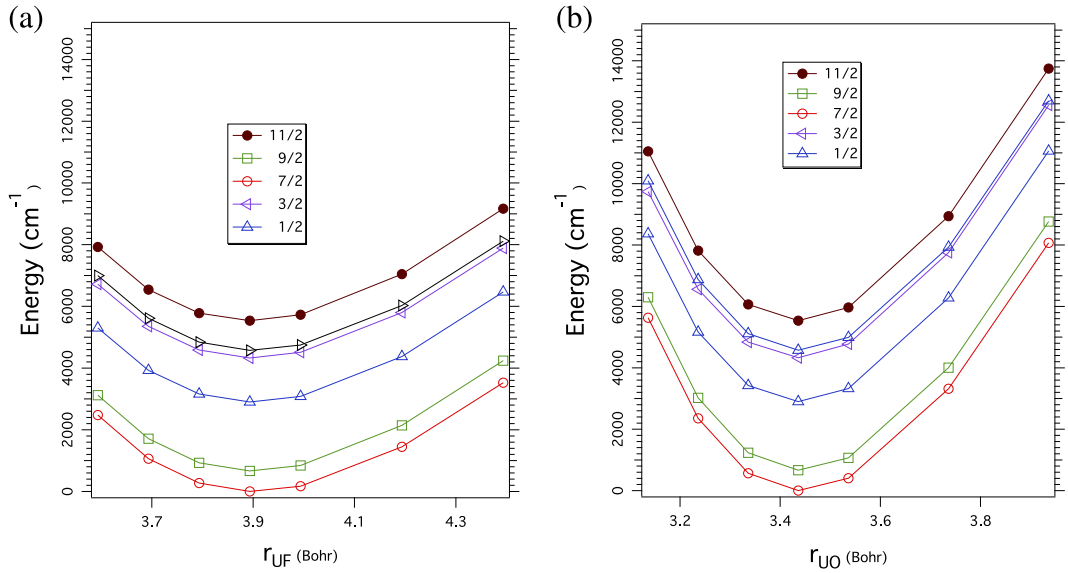

FIG. 5. The SO-CASPT2/CBS(PP) potential energy curves of the lowest six Ω states for UFO along (a) R_{UF} and (b) R_{UO}.

The first excited state of UFO (Ω = 9/2), which lies at 561 cm^{-1} (0.069 eV) above the ground state, is a strong mixture of two SR states (52% $(1)^2H$ + 36% $(1)^4H$) and both of these arise from the same configuration (1φ1δ3σ). The calculated second VDE associated with this latter state is 1.359 eV (1.29 eV + 0.069 eV), which is 0.041 eV lower than the experimental value, and corresponds to peak A in the experimental spectra (Figure 4). The calculated X-A separation is 0.069 eV, in comparison to the experimental value of 0.11 eV. However, the observed peak following A that corresponds to a vibrational progression of frequency 645 cm^{-1} is calculated at the SO-CASPT2/VQZ-PP level (see below) to correspond to the UF stretch but is strongly underestimated at 542 cm^{-1} at this level of theory (DKH-CASPT2 without SO yields a frequency of 536 cm^{-1}). The observed third VDE corresponds to the weak and broad band B at 1.84 eV (Figure 4). There are several candidates to assign for this peak, including the calculated value of 1.788 eV. This state is an Ω = 11/2 and is 92% ^4K (1φ1δ2δ), which corresponds to the $5f^26d$ configuration of U. The VDE of the next broad band C occurs at 2.04 eV, which could be assigned to several calculated states between 1.8 and 2.3 eV. For example, the calculated value at 2.279 eV, Ω = 5/2, is a strong mixture of $^2\Phi$, $^4\Phi$, $^4\Gamma$ (2) SR states, where most of these also correlate to the $5f^26d$ configuration of U. In the 266 nm spectrum, another weak broad band D at VDE of 2.42 eV has been observed experimentally. There is an excellent agreement of the experimental value with that of the calculated value of 2.422 eV. This electronic state (Ω = 1/2) is also a strong SO mixing of several SR states like $a^2\Sigma^-$ (44%), $a^4\Sigma^-$ (28%), $b^2\Pi$ (14%), and $a^4\Delta$ (4%), which originate from different configurations, as shown in Table II, but all are associated with the $5f^27s$ configuration of U. There are, however, several other nearby states within 0.2 eV that could be assigned to this feature and the present calculations are not sufficient to make a definitive assignment. The configurational assignments[62,63] of spin-free and SO states are shown in the supplementary material (Tables S1-S4).[64]

The weak features B, C, and D correspond to two-electron transition processes (shake-up bands), that is, they have been accessed from the ground state configuration of UFO^- [X^3H $(3\sigma)^2(1\varphi)^1(1\delta)^1$] via two-electron transitions, in which one electron has been detached from one of these orbitals and simultaneously another electron has been excited to another higher unoccupied 5f or 6d orbital of U. As shown in Table III, many detachment transitions due to two-electron transitions contribute these broad and weak PES bands. There are also almost continuous and weak PES features in the 266 nm spectrum beyond 2.50 eV (Figure 4(b)). These features were not resolved due to the low spectral resolution and a high density of electronic states, mostly due to two-electron transitions. These transitions calculated theoretically have been listed in Table III.

Table III lists a manifold of many low-lying SO excited states of UFO with their Ω values, the configurational assignments of the contributed SR states, the excitation energies, and also the VDEs. It has been found that in most cases, there are strong SO mixing of several SR spin-free states of different contributions and these states are placed energetically very close to each other. In many cases, the differences in energies between the coupled states are below 0.03 eV. Therefore, the strong configuration mixing as well as the strong relativistic effects results in the complexity of excited electronic states of UFO and also the photoelectron spectra of UFO^-. This triatomic UFO^- species together with previously investigated UO_2^- species is examples of challenging cases, where strong electron correlation and relativistic effects make the calculations and interpretations of the PES and excited states very difficult.

Calculated equilibrium geometries and stretching harmonic frequencies for the low-lying Ω states of UFO are reported in Table IV. Most of the states shown arise from the

TABLE IV. SO-CASPT2/CBS(-PP) molecular properties of UFO for selected Ω states.

Ω State	ΔE[a] (eV)	T_e[b] (cm^{-1})	r_e (UO) (Å)	r_e (UF) (Å)	ω_1[c] (cm^{-1})	ω_3[c] (cm^{-1})
(X) 7/2	1.290	0	1.809	2.054	890	536
(1) 9/2	1.372	636	1.810	2.052	894	544
(1) 1/2	1.632	2749	1.810	2.054	887	538
(1) 3/2	1.802	4107	1.809	2.055	888	535
(2) 1/2	1.825	4326	1.810	2.054	888	536
(1) 11/2	1.824	4681	1.826	2.098		
(2) 9/2	1.970	5450	1.809	2.052	892	540
(2) 11/2	1.980	5494	1.807	2.049		
(2) 3/2	2.340	8432	1.808	2.054	888	538
(3) 1/2	2.347	8482	1.808	2.053	891	536
(1) 5/2	2.298	8539	1.825	2.092		
(2) 5/2	2.340	8685	1.817	2.086		
(1) 13/2	2.319	8654	1.823	2.093	861	505
(4) 1/2	2.382	8791	1.810	2.052	886	537
(3) 3/2	2.378	9022	1.817	2.071	859	496
(2) 7/2	2.420	9495	1.828	2.098		
(3) 5/2	2.421	9444	1.822	2.086		
(2) 13/2	2.541	9994	1.806	2.049	890	530
(3) 11/2	2.602	10479	1.807	2.047	894	543
(5) 1/2	2.608	10531	1.807	2.047	890	540
(4) 3/2	2.565	10585	1.822	2.083		

[a]Vertical detachment energy of UFO^- shifted to match the experimental first VDE of 1.29 eV. The SO-CASPT2/CBS(-PP) value for the 1st VDE is 1.234 eV.
[b]Equilibrium excitation energies of neutral UFO.
[c]Stretching vibrational frequencies of UFO. ω_1 and ω_3 correspond to primarily the UO and UF stretches, respectively.

$5f^2 7s$ configuration and have very similar geometries and harmonic frequencies, with r_e(UO) ~ 1.81 Å, r_e(UF) ~ 2.06 Å, ω_1 at ~890 cm^{-1}, and ω_3 at ~530 cm^{-1}. A few of the states shown correspond to contributions from the $5f^2 6d$ configuration, and these are marked by bond lengths that are longer by about 0.02 Å and 0.04 Å for the UO and UF distances, respectively, with correspondingly smaller vibrational frequencies. Most of these potential energy surfaces were heavily perturbed, however, which made their resulting harmonic frequencies too uncertain to list in Table IV since the fits to Eq. (3) were not of sufficient accuracy.

IV. CONCLUDING REMARKS

We report the first experimental observation of the UFO^- anion, as well as extensive relativistic quantum chemistry calculations to understand the electronic structure of UFO^- and UFO. The electron affinity of UFO was matured to be 1.27(3) eV. But the photoelectron spectra were quite complicated and UFO represents an extremely challenging electronic system from a theoretical point of view. Strong electron correlation and SO coupling effects were found and they led to a high density of electronic states with strong configurational mixings. Therefore, the assignments of many of the excited states are somewhat tentative.

ACKNOWLEDGMENTS

We are grateful to Professor Dr. W. H. Eugen Schwarz for helpful discussions. The experimental material was based on work supported by the U.S. Department of Energy, Office of Science, Office of Basic Energy Sciences, Heavy Element Chemistry Program through Grant No. DE-SC0006979 (L.S.W.). The DKH-based theoretical work was supported by NSF of China under Grant Nos. 91426302 and 21433005 (J.L.). The latter calculations were performed using the Tsinghua National Laboratory for Information Science and Technology. The PP-based theoretical work was supported by the U.S. Department of Energy Office of Science, Office of Basic Energy Sciences, Heavy Element Chemistry Program through Grant No. DE-FG02-12ER16329 (K.A.P.).

[1]C. R. Edwards and A. J. Oliver, "Uranium processing: A review of current methods and technology," JOM **52**(9), 12–20 (2000).
[2]E. Biémont, P. Palmeri, P. Quinet, Z. G. Zhang, and S. Svanberg, Astrophys. J. **567**, 1276 (2002).
[3]L. Gagliardi and B. O. Roos, Chem. Soc. Rev. **36**, 893 (2007).
[4]P. Pyykkö, Chem. Rev. **88**, 563 (1988).
[5]B. O. Roos and P.-Å. Malmqvist, Phys. Chem. Chem. Phys **6**, 2919 (2004).
[6]M. Barysz and Y. Ishikawa, *Challenges and Advances in Computational Chemistry and Physics* (Springer, 2010).
[7]S. D. Gabelnick, G. T. Reedy, and M. G. Chasanov, J. Chem. Phys. **58**, 4468 (1973).
[8]R. D. Hunt and L. Andrews, J. Chem. Phys. **98**, 3690 (1993).
[9]M. F. Zhou, L. Andrews, N. Ismail, and C. Marsden, J. Phys. Chem. A **104**, 5495 (2000).
[10]L. Gagliardi, B. O. Roos, P. A. Malmqvist, and J. M. Dyke, J. Phys. Chem. A **105**, 10602 (2001).
[11]J. D. Han, L. A. Kaledin, V. Goncharov, A. V. Komissarov, and M. C. Heaven, J. Am. Chem. Soc. **125**, 7176 (2003).
[12]J. D. Han, V. Goncharov, L. A. Kaledin, A. V. Komissarov, and M. C. Heaven, J. Chem. Phys. **120**, 5155 (2004).
[13]C. J. Lue, J. Jin, M. J. Ortiz, J. C. Rienstra-Kiracofe, and M. C. Heaven, J. Am. Chem. Soc. **126**, 1812 (2004).
[14]J. Li, B. E. Bursten, L. Andrews, and C. J. Marsden, J. Am. Chem. Soc. **126**, 3424 (2004).
[15]C. Clavaguera-Sarrio, V. Vallet, D. Maynau, and C. J. Marsden, J. Chem. Phys. **121**, 5312 (2004).

[16]R. Tyagi, Ph.D. thesis, Ohio State University, 2005.
[17]L. Gagliardi, M. C. Heaven, J. W. Krogh, and B. O. Roos, J. Am. Chem. Soc. **127**, 86 (2005).
[18]T. Fleig, H. J. A. Jensen, J. Olsen, and L. Visscher, J. Chem. Phys. **124**, 104106 (2006).
[19]I. Infante, E. Eliav, M. J. Vilkas, Y. Ishikawa, U. Kaldor, and L. Visscher, J. Chem. Phys. **127**, 124308 (2007).
[20]J. M. Merritt, J. Han, and M. C. Heaven, J. Chem. Phys. **128**, 084304 (2008).
[21]I. Infante, L. Andrews, X. F. Wang, and L. Gagliardi, Chem. - Eur. J. **16**, 12804 (2010).
[22]W. L. Li, H. S. Hu, T. Jian, G. V. Lopez, J. Su, J. Li, and L. S. Wang, J. Chem. Phys. **139**, 244303 (2013).
[23]W. L. Li, J. Su, T. Jian, G. V. Lopez, H. S. Hu, G. J. Cao, J. Li, and L. S. Wang, J. Chem. Phys. **140**, 094306 (2014).
[24]J. Czekner, G. V. Lopez, and L. S. Wang, J. Chem. Phys. **141**, 244302 (2014).
[25]L. S. Wang, H. S. Cheng, and J. W. Fan, J. Chem. Phys. **102**, 9480 (1995).
[26]K. Andersson, F. Aquilante, A. Bernhardsson, M. R. A. Blomberg, J. Boström *et al.*, MOLCAS version 7.8, Department of Theoretical Chemistry, Chemical Centre, University of Lund, Sweden, 2012.
[27]B. A. Hess, Phys. Rev. A **33**, 3742 (1986).
[28]B. O. Roos, R. Lindh, P.-Å. Malmqvist, V. Veryazov, and P.-O. Widmark, Chem. Phys. Lett. **409**, 295 (2005).
[29]M. Dolg and X. Cao, J. Phys. Chem. A **113**, 12573 (2009).
[30]K. A. Peterson, J. Chem. Phys. **142**, 074105 (2015).
[31]T. H. Dunning, Jr., J. Chem. Phys. **90**, 1007 (1989).
[32]R. A. Kendall, T. H. Dunning, Jr., and R. J. Harrison, J. Chem. Phys. **96**, 6796 (1992).
[33]I. Infante and L. Visscher, J. Chem. Phys. **121**, 5783 (2004).
[34]I. O. Antonov and M. C. Heaven, J. Phys. Chem. A **117**, 9684 (2013).
[35]D. H. Bross and K. A. Peterson, J. Chem. Phys. **143**, 184313 (2015).
[36]F. Réal, A. S. P. Gomes, L. Visscher, V. Vallet, and E. Eliav, J. Phys. Chem. A **113**, 12504 (2009).
[37]K. Pierloot and E. van Besien, J. Chem. Phys. **123**, 204309 (2005).
[38]A. Karton and J. M. L. Martin, Theor. Chem. Acc. **115**, 330 (2006).
[39]D. H. Bross and K. A. Peterson, J. Chem. Phys. **141**, 244308 (2014).
[40]J. M. L. Martin, Chem. Phys. Lett. **259**, 669 (1996).
[41]D. Feller, K. A. Peterson, and J. G. Hill, J. Chem. Phys. **135**, 044102 (2011).
[42]J. P. Perdew, K. Burke, and M. Ernzerhof, Phys. Rev. Lett. **77**, 3865 (1996).
[43]E. van Lenthe, E. J. Baerends, and J. G. Snijders, J. Chem. Phys. **99**, 4597 (1993).
[44]ADF 2010.02, SCM, Vrije Universiteit, Amsterdam, see http://www.scm.com.
[45]C. F. Guerra, J. G. Snijders, G. te Velde, and E. J. Baerends, Theor. Chem. Acc. **99**, 391 (1998).
[46]G. te Velde, F. M. Bickelhaupt, E. J. Baerends, C. F. Guerra, S. J. A. Van Gisbergen, J. G. Snijders, and T. J. Ziegler, J. Comput. Chem. **22**, 931 (2001).
[47]E. van Lenthe and E. J. Baerends, J. Comput. Chem. **24**, 1142 (2003).
[48]J. Li and B. E. Bursten, J. Am. Chem. Soc. **119**, 9021 (1997).
[49]E. J. Baerends, D. E. Ellis, and P. Ros, Chem. Phys. **2**, 42 (1973).
[50]G. Ghigo, B. O. Roos, and P.-Å. Malmqvist, Chem. Phys. Lett. **396**, 142 (2004).
[51]B. A. Hess, C. M. Marian, U. Wahlgren, and O. Gropen, Chem. Phys. Lett. **251**, 365 (1996).
[52]O. Christiansen, J. Gauss, and B. Schimmelpfennig, Phys. Chem. Chem. Phys. **2**, 965 (2000).
[53]P.-Å. Malmqvist, B. O. Roos, and B. Schimmelpfenning, Chem. Phys. Lett. **357**, 230 (2002).
[54]H.-J. Werner, P. J. Knowles, G. Knizia, F. R. Manby, M. Schütz *et al.*, MOLPRO, version 2012.1, a package of *ab initio* programs, 2012, see http://www.molpro.net.
[55]P. Celani and H.-J. Werner, J. Chem. Phys. **112**, 5546 (2000).
[56]A. Berning, M. Schweizer, H.-J. Werner, P. J. Knowles, and P. Palmieri, Mol. Phys. **98**, 1823 (2000).
[57]J. Senekowitsch, Ph.D. thesis, Universität Frankfurt, 1988.
[58]P. F. Bernath, *Spectra of Atoms and Molecules*, 2nd ed. (Oxford University Press, 2005).
[59]E. D. Glendening, J. K. Badenhoop, A. E. Reed, J. E. Carpenter, J. A. Bohmann, C. M. Morales, C. R. Landis, and F. Weinhold, NBO 6.0., Theoretical Chemistry Institute, University of Wisconsin, Madison, WI, 2013, http://nbo6.chem.wisc.edu/.
[60]P. Atkins and R. Friedman, *Molecular Quantum Mechanics*, 4th ed. (Oxford University Press, 2005).
[61]*Reviews in Computational Chemistry*, edited by K. B. Lipkowitz and D. B. Boyd (John Wiley & Sons, 2001), Vol. 17.
[62]G. Herzberg, *Textbook of Molecular Spectra and Molecular Structure: Spectra of Diatomic Molecules*, 2nd ed. (Van Nostrand, 1963).
[63]K. Balasubramanian, *Relativistic Effects in Chemistry. Part A. Theory and Techniques* (John Wiley & Sons, 1997).
[64]See supplementary material at http://dx.doi.org/10.1063/1.4942188 for Tables S1-S5.